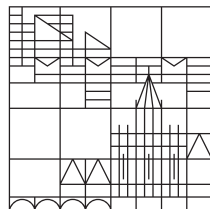


# Optical signature of magnetic phase transitions in transition metal thiophosphates

Bachelor Thesis of Leon Oleschko  
supervised by Dr. Mateusz Goryca

February 9, 2024

Universität  
Konstanz



UNIVERSITY  
OF WARSAW

## Literature Review: Oct 2023

### Current Status

Materials

Setup

Photoluminescence and Reflection at 0 T

NiPS<sub>3</sub> in magnetic field

in plane

out of plane

CrPS<sub>4</sub>

### Writing

## Search Terms

- ▶ transition metal phosphor sulfates OR FePS3 OR NiPS3 OR CrPS4 OR MnPS3
- ▶ spectroscopy of transition metal phosphor sulfates OR FePS3 OR NiPS3 OR CrPS4 for magnetic field
- ▶ magnetic order OR magnetic phase in semiconductor AND spectroscopy
- ▶ kerr OR moke OR Magnetic Circular Dichroism Spectroscopy

# Magnetic Structure and Metamagnetic Transitions in the van der Waals Antiferromagnet CrPS<sub>4</sub> - 1/3

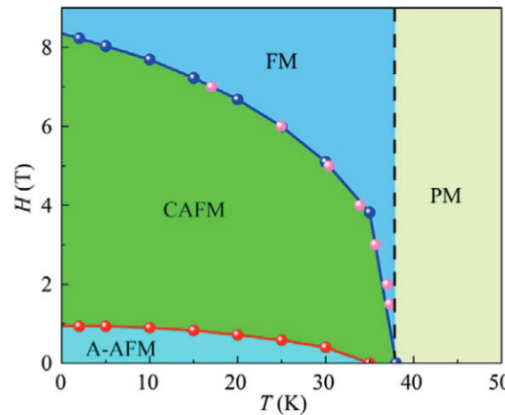
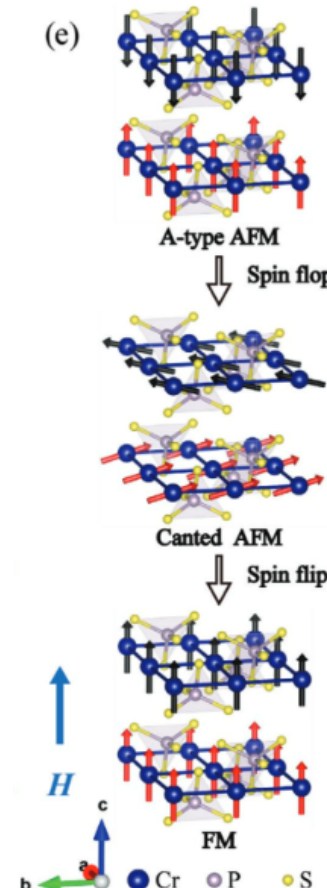


**Figure 5.** Magnetic phase diagram of CrPS<sub>4</sub> with applied field along the  $c$  axis. The red and blue balls are extracted from the  $M(H)$  curves shown in Figure 2. Pink balls are extracted from the  $M(T)$  curves. The black dashed line is for a potential boundary between the FM and PM phases at  $T_N = 38$  K.

A-AFM:  $\vec{m} \parallel \vec{n}_{\text{lattice}} = \vec{c}$   
C-AFM:  $\vec{m} \nparallel \vec{c}$  (canted)



# Magnetic Structure and Metamagnetic Transitions in the van der Waals Antiferromagnet CrPS<sub>4</sub> - 2/3

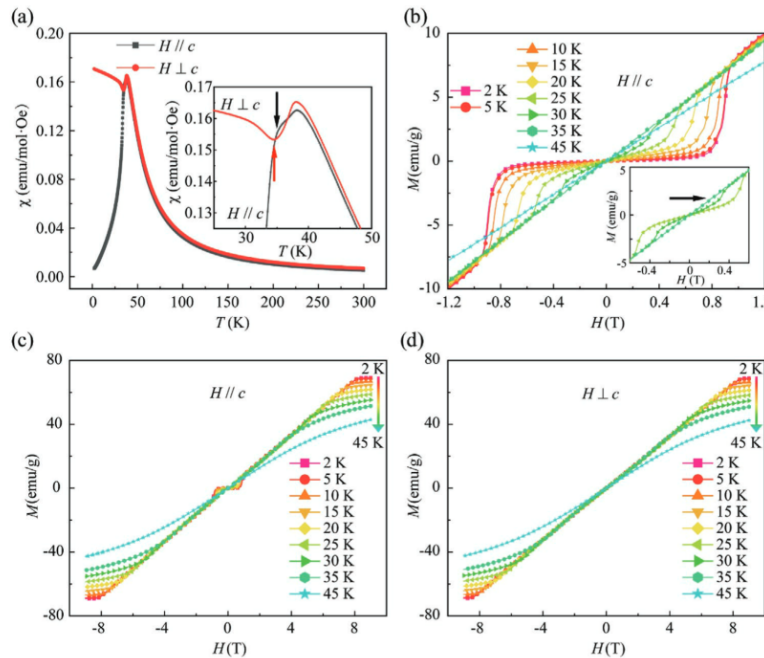
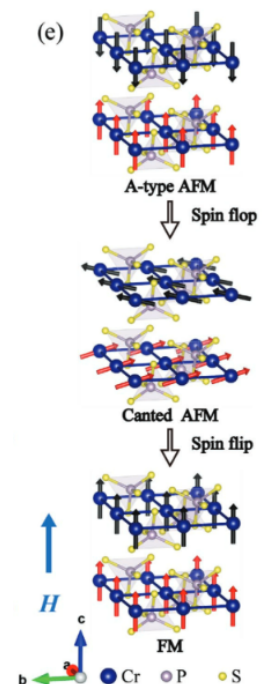


**Figure 2.** a) Zero-field-cooled magnetic susceptibilities of CrPS<sub>4</sub> single crystal with 1 kOe field applied in parallel and perpendicular to the crystallographic  $c$  axis. Inset shows the zoom-in image of observed anomalies around 35 K. b,c) Field-dependent magnetization at different temperatures with field parallel to the  $c$  axis. The inset of (b) shows the zoom-in image of the absent spin-flop transition at 35 K indicated by the black arrow. d) Field-dependent magnetization at different temperatures with field perpendicular to the  $c$  axis.

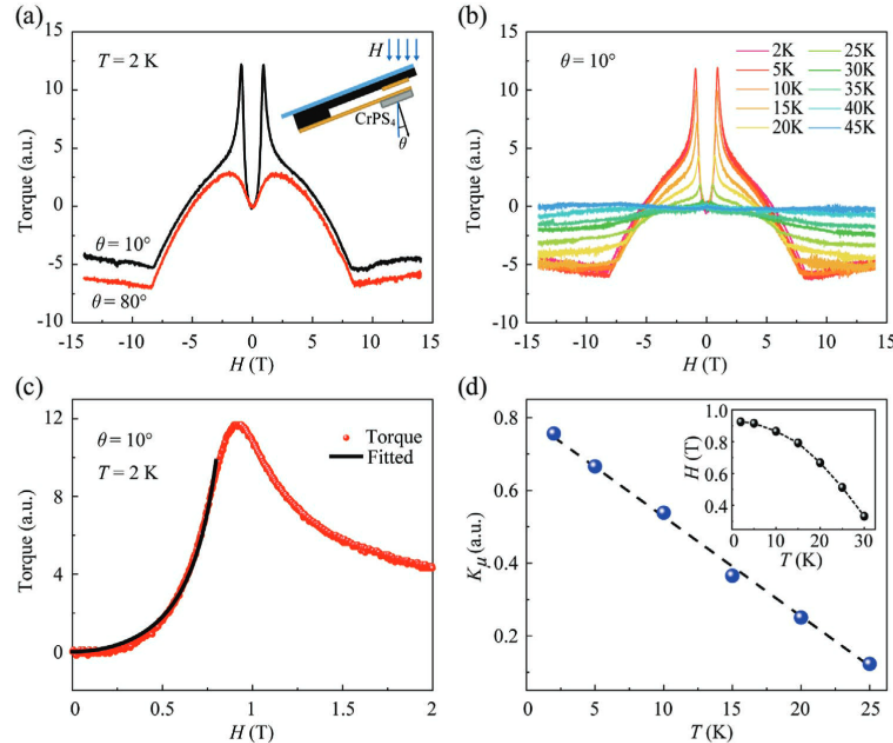


$\theta = \angle(\vec{c}, \vec{H})$  is important!

$\chi(B \approx 0, T \approx 0) \approx 0$  is a property of AFM?

A-AFM – C-AFM transition based on  $\frac{dM}{dH}$  (b)

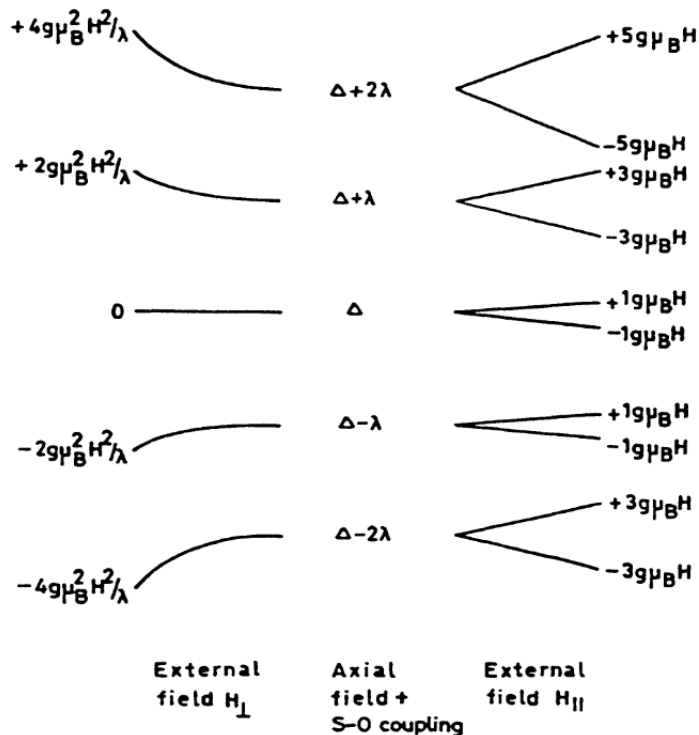
# Magnetic Structure and Metamagnetic Transitions in the van der Waals Antiferromagnet CrPS<sub>4</sub> - 3/3 Torque



C-AFM – FM transition based on  
 $\frac{d^2\text{Torque}}{dH^2}$  (a,b)

**Figure 3.** a) Magnetic torque of  $\theta = 10^\circ$  and  $80^\circ$  at  $2$  K. The schematic diagram of the measurement is shown in the inset. b) Magnetic torque of  $\theta = 10^\circ$  at different temperatures. The sharp torque peaks correspond to spin-flop transitions, allowing  $H_{SF}(T)$  to be determined precisely. c) Low-field torque of  $\theta = 10^\circ$  at  $2$  K and the fitting result by using Equation (2). d) The fitted anisotropy energy  $K_\mu$  of  $\theta = 10^\circ$  using data in (b). The dashed line is the linear fitting of the anisotropy energy. Inset: the spin-flop fields at different temperature extracted from (b).

# Magnetism in the layered transition-metal thiophosphates MPS3



Heisenberg model  $\Rightarrow$  different splitting for different  $\angle(\vec{H}, \vec{n})$

FIG. 7. Energy levels corresponding to  $S=2$  for the Hamiltonian (4) in the absence of an external field ( $H=0$ ), with the applied field parallel to the trigonal axis ( $H=H_{\parallel}$ ) and with the field perpendicular to the trigonal axis ( $H=H_{\perp}$ ).

# Magnetization Study of the AFM-FM Coexistence in the Manganite System



Coexistence of AFM in the bulk interior and FM at the surface

⇒ Different behaviour in Kerr (surface) and Faraday?

For the manganites  $\text{Pr}_{0.5}\text{Ca}_{0.5-x}\text{Sr}_x\text{MnO}_3$  ( $x = 0; 0.3$ ) the temperature and cooling field dependence of the reduced remanence asymmetry indicates the antiferromagnetic exchange between the antiferromagnetic and ferromagnetic spins at the surface of the clusters. For  $x = 0.3$  we deduce the radius of the cluster in the field cooled regime to be about 20 times larger than that for  $x = 0$ .

# Field-dependent magneto-optical Kerr effect spectroscopy applied to the magnetic component diagnosis of a rubrene/Ni system

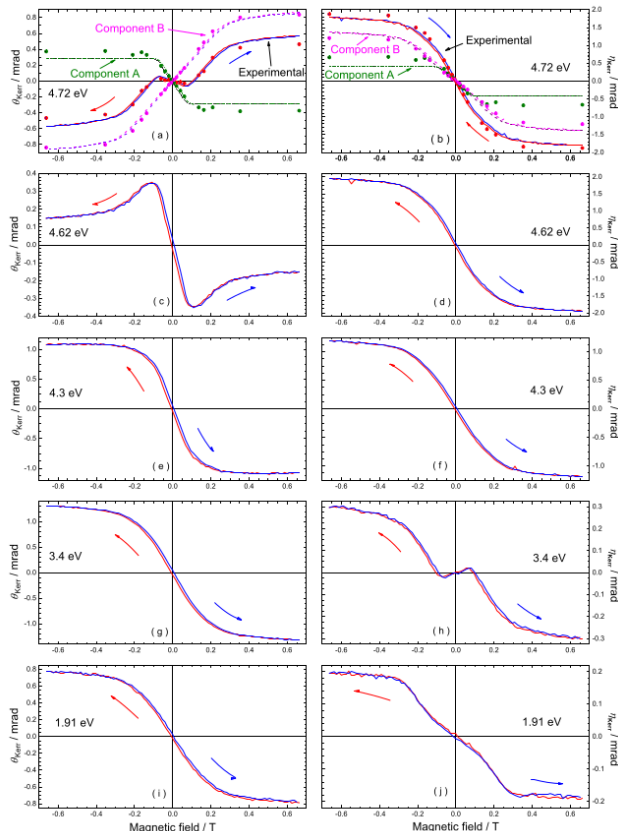


Fig. 2. (a-j) Hysteresis measured by polar MOKE at RT and at various photon energies. The left and right panels show the real part (rotation) and the imaginary part (ellipticity), respectively, of the complex MOKE signal.

Rubrene: organic semiconductor

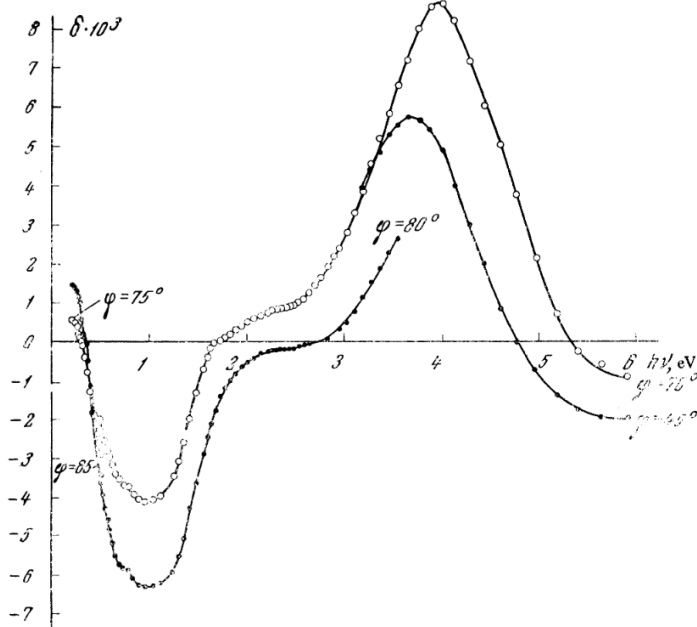
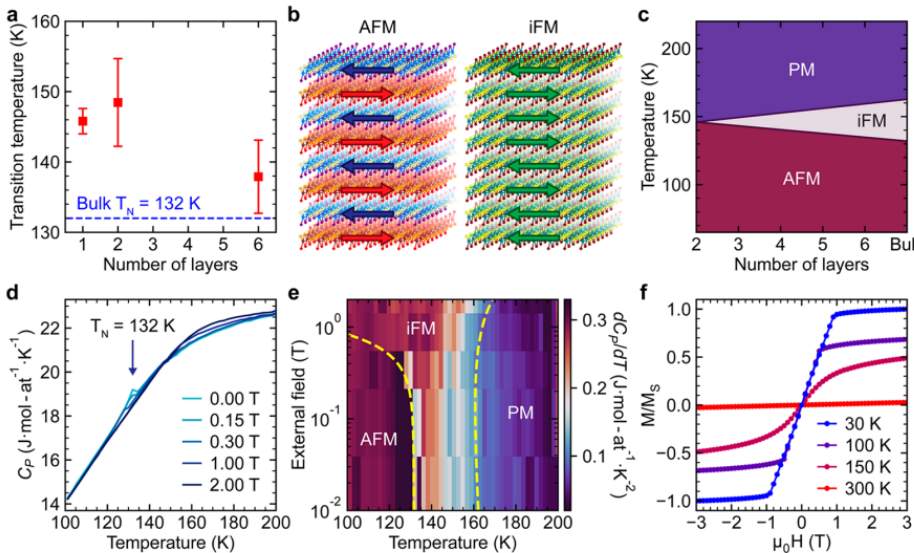


FIG. 2. Equatorial Kerr effect of Ni for two angles of incidence of light.

# Magnetic Order and Symmetry in the 2D Semiconductor CrSBr



**Figure 4.** (a) Magnetic phase transition temperature as a function of layer number, probed by SHG. (b) Structures of AFM and iFM phases in bulk CrSBr at zero field. (c) Schematic magnetic phase diagram presented as a function of layer number and temperature. (d) Heat capacity of bulk CrSBr as a function of temperature at different applied magnetic fields. The curves show a sharp AFM transition at 132 K and a broad feature around 160 K assigned to intralayer FM ordering. The external field is applied along the  $c$ -axis. (e) Magnetic phase diagram of bulk CrSBr, as determined from  $C_p$  measurements. The yellow dashed lines are guides to the eye to distinguish the different magnetic phases. (f) Magnetization versus applied magnetic field at  $T = 30, 100, 150, \text{ and } 300$  K.  $M$  is normalized to the saturation magnetization value at  $T = 50$  K. The magnetic field is applied along the  $a$ -axis. Data in part e are reproduced from ref 29.

## Literature Review: Oct 2023

### Current Status

Materials

Setup

Photoluminescence and Reflection at 0 T

NiPS<sub>3</sub> in magnetic field

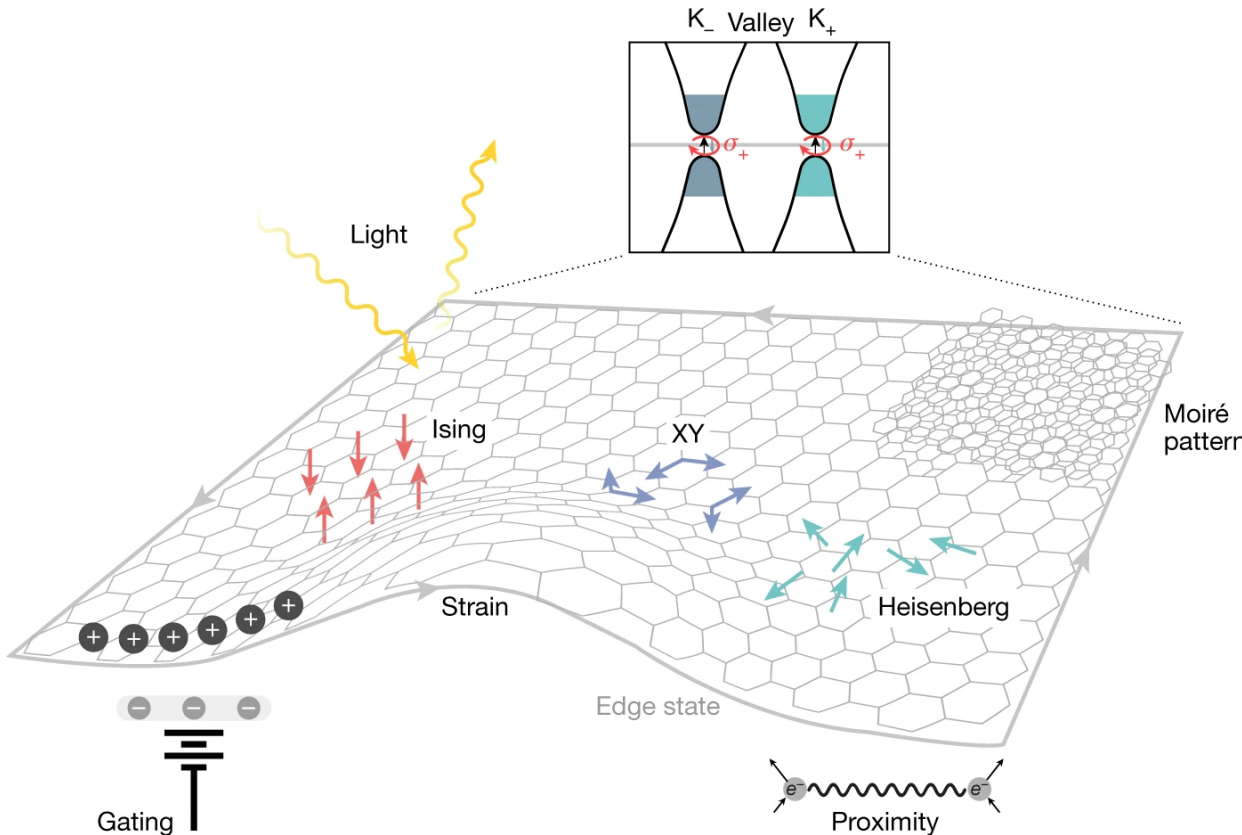
in plane

out of plane

CrPS<sub>4</sub>

Writing

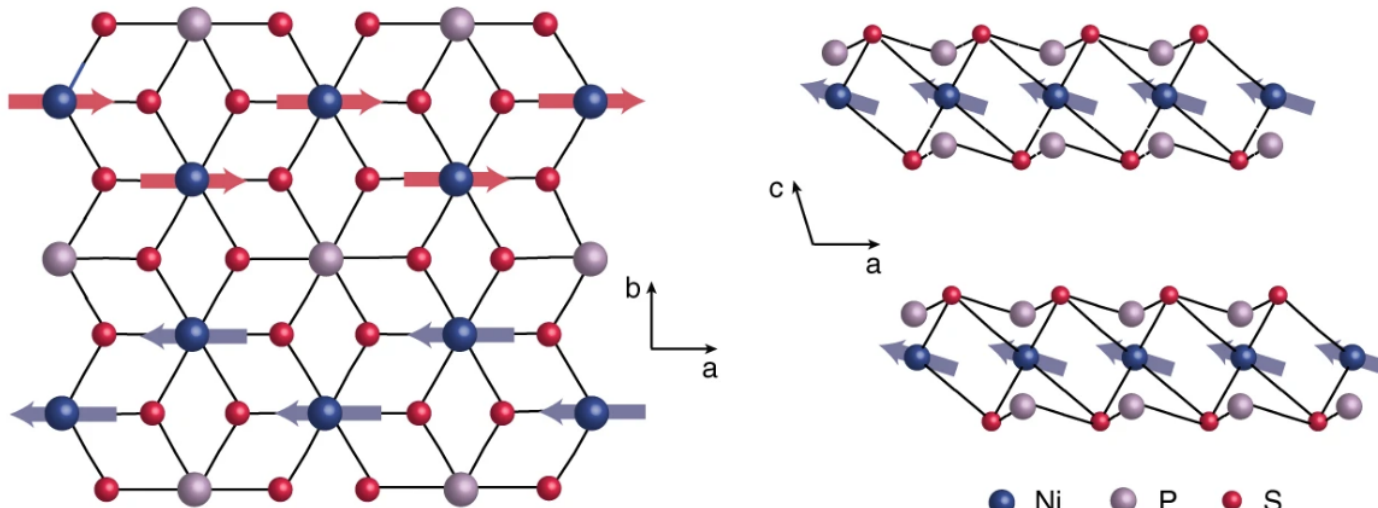
# Magnetism in van der Waals materials



Magnetism in two-dimensional van der Waals materials, Nature 2018

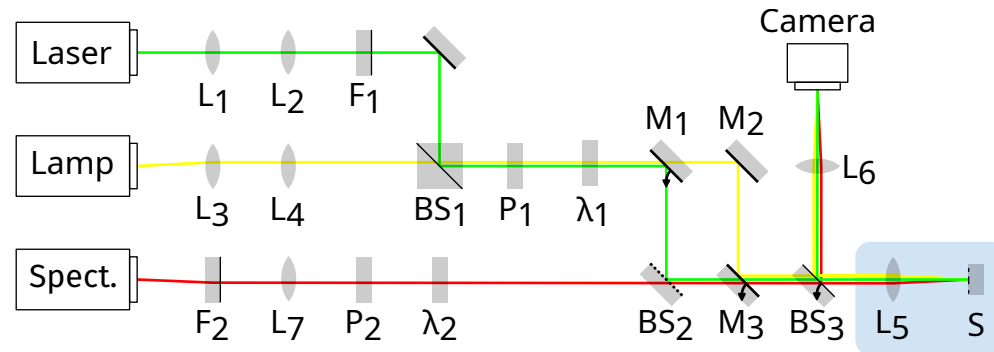
"While **MnPS<sub>3</sub>** is best described by the **isotropic Heisenberg Hamiltonian**, **FePS<sub>3</sub>** is most effectively treated by the **Ising model**, while **NiPS<sub>3</sub>** is best described by the **anisotropic Heisenberg Hamiltonian**."

Magnetism in the layered transition-metal thiophosphates MPS<sub>3</sub> (M = Mn, Fe, and Ni), Physical Review B 1992

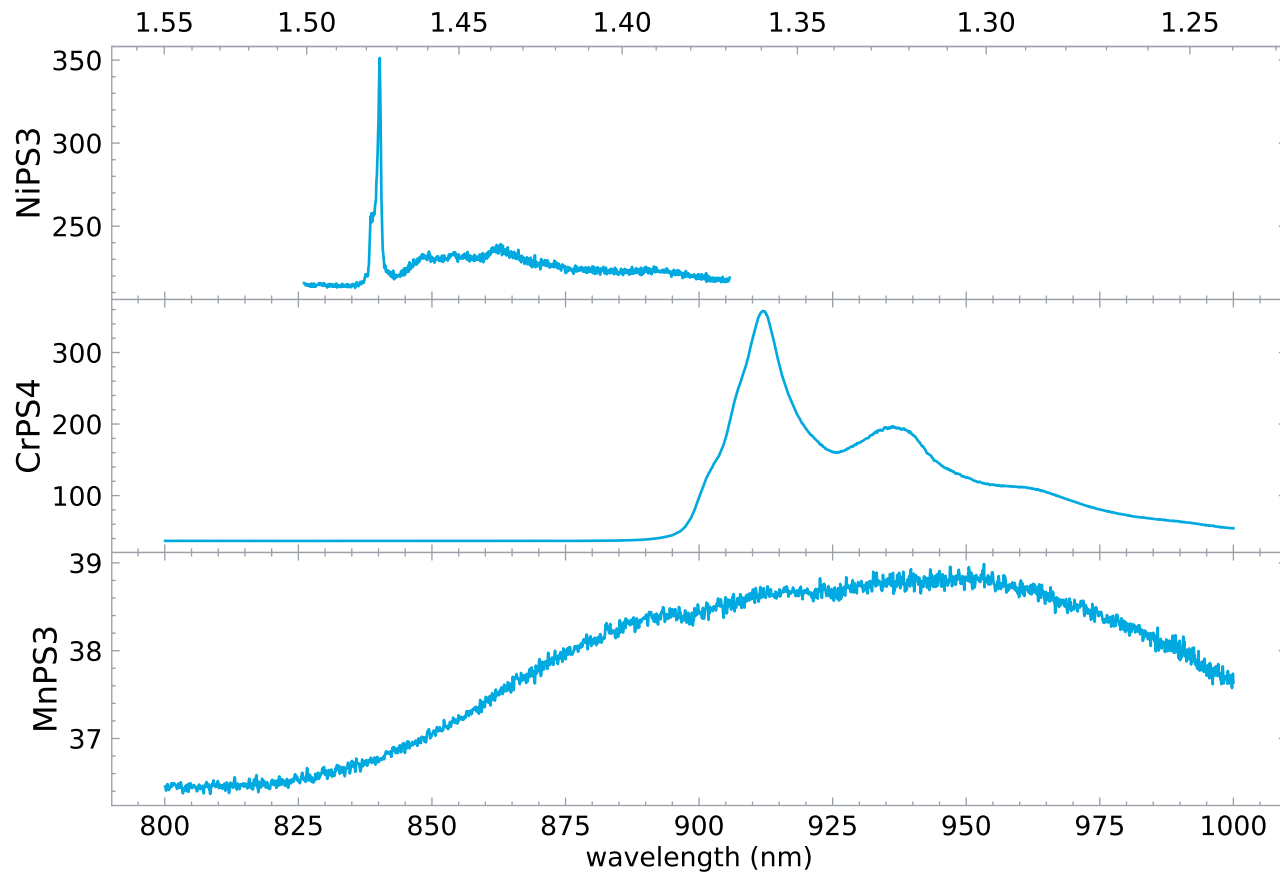


Exciton-driven antiferromagnetic metal in a correlated van der Waals insulator, Nature Communications 2021

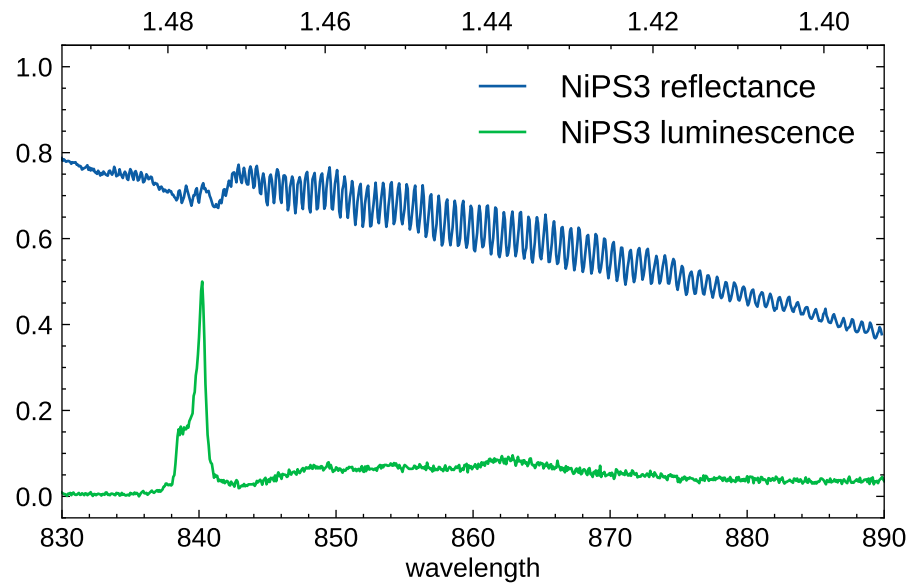
# Setup

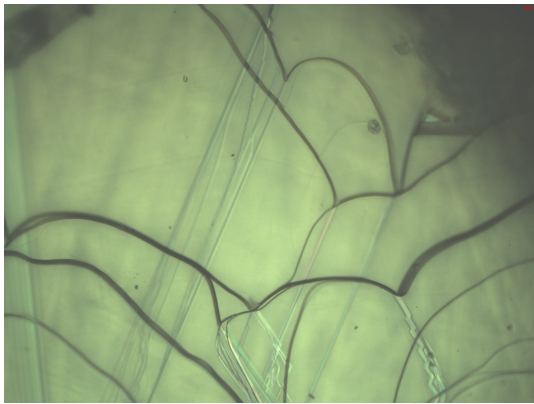


# bulk PL spectra at 10 K

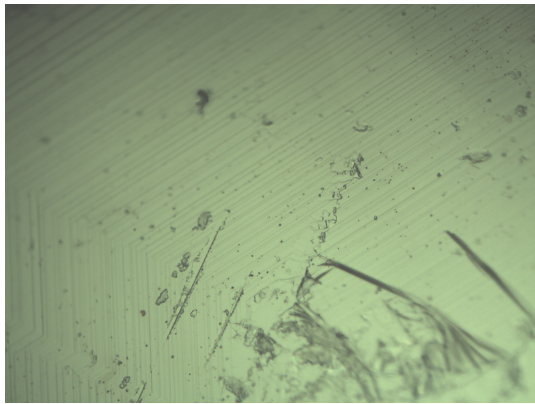


## Reflectance spectra





MnPS<sub>3</sub> Bulk Crystal (50x)



NiPS<sub>3</sub> Bulk Crystal (50x)



NiPS<sub>3</sub> Exfoliated Crystal

## Literature Review: Oct 2023

### Current Status

Materials

Setup

Photoluminescence and Reflection at 0 T

**NiPS<sub>3</sub> in magnetic field**

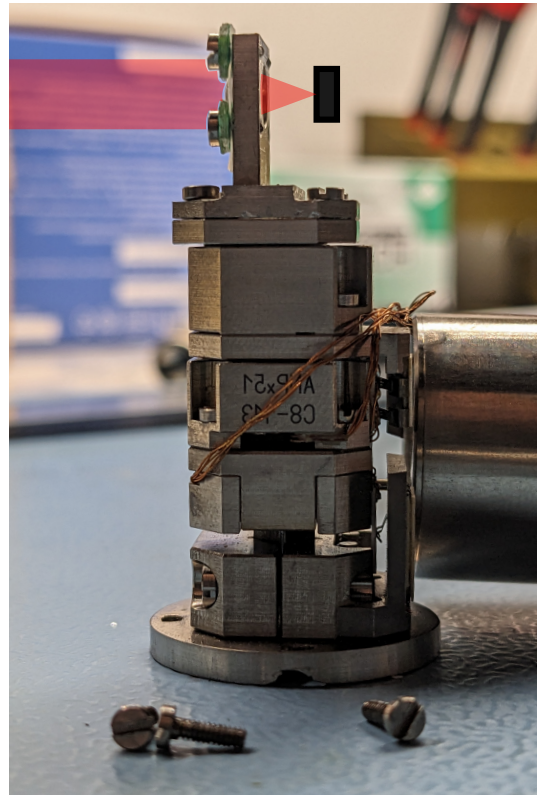
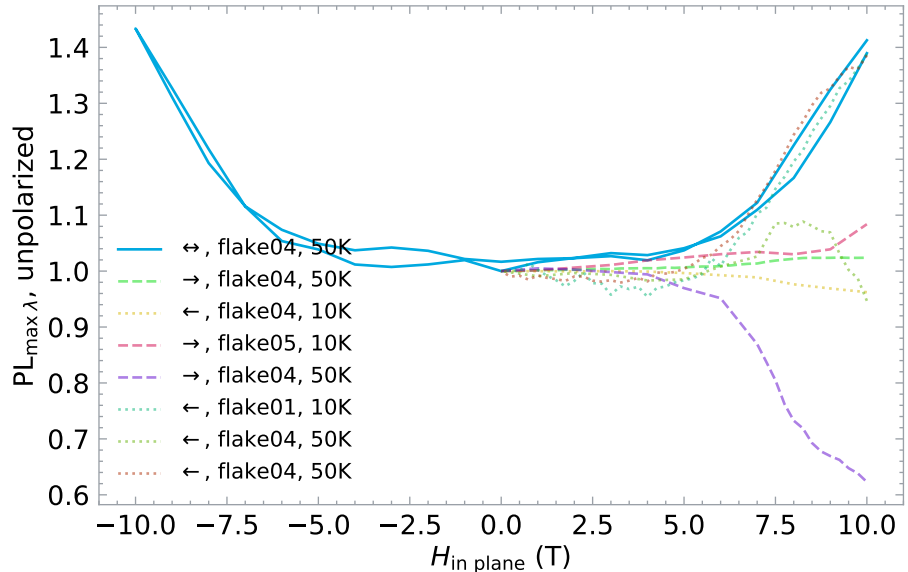
in plane

out of plane

CrPS<sub>4</sub>

### Writing

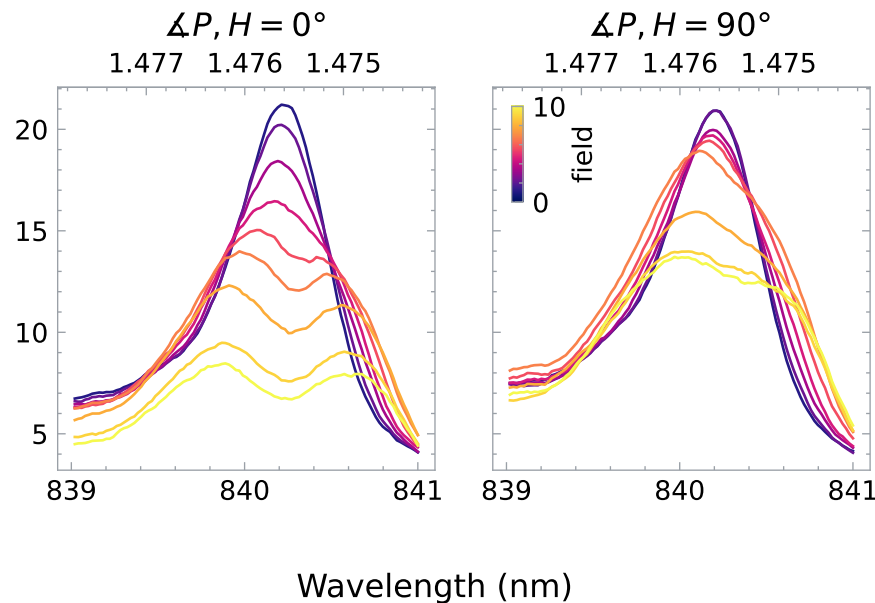
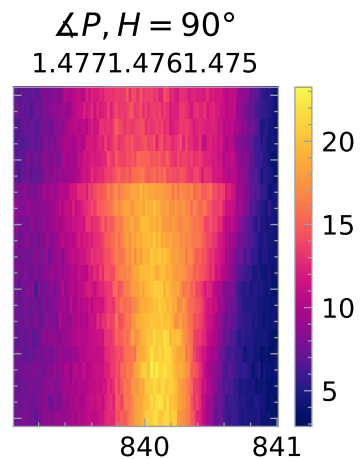
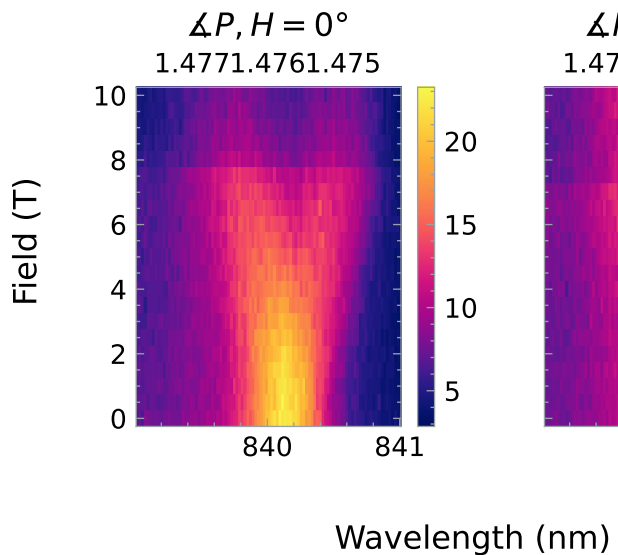
# Instability of the Lens assembly?



Field in plane of the image.

# Splitting of the PL peak at $\Delta P, H = 0$

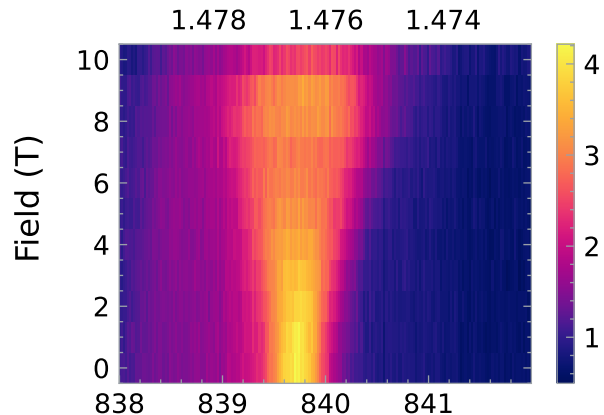
2023-12-22\_NiPS3\_inPlane/d002\_circPolExc\_linDetPol\_5K\_flake01\_1mW



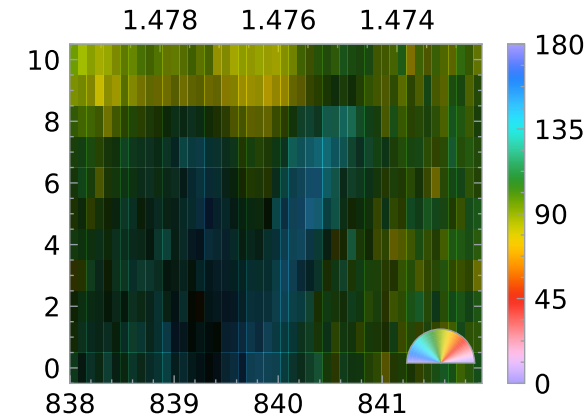
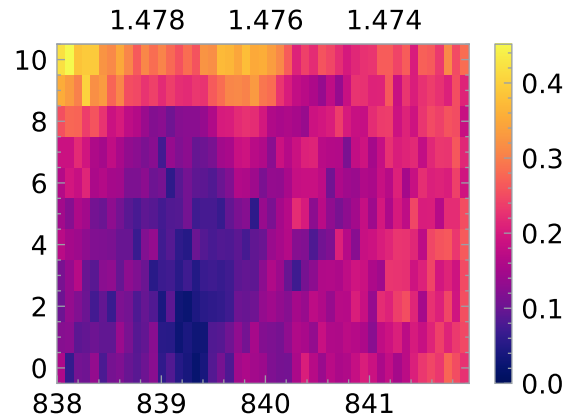
# Polarisation

2023-12-06\_LO\_MG\_NiPS3/d004\_10K\_647nm\_rotPolDet\_flake05\_sweepDown\_inPlane.hd5

normalized PL, all Polarisations



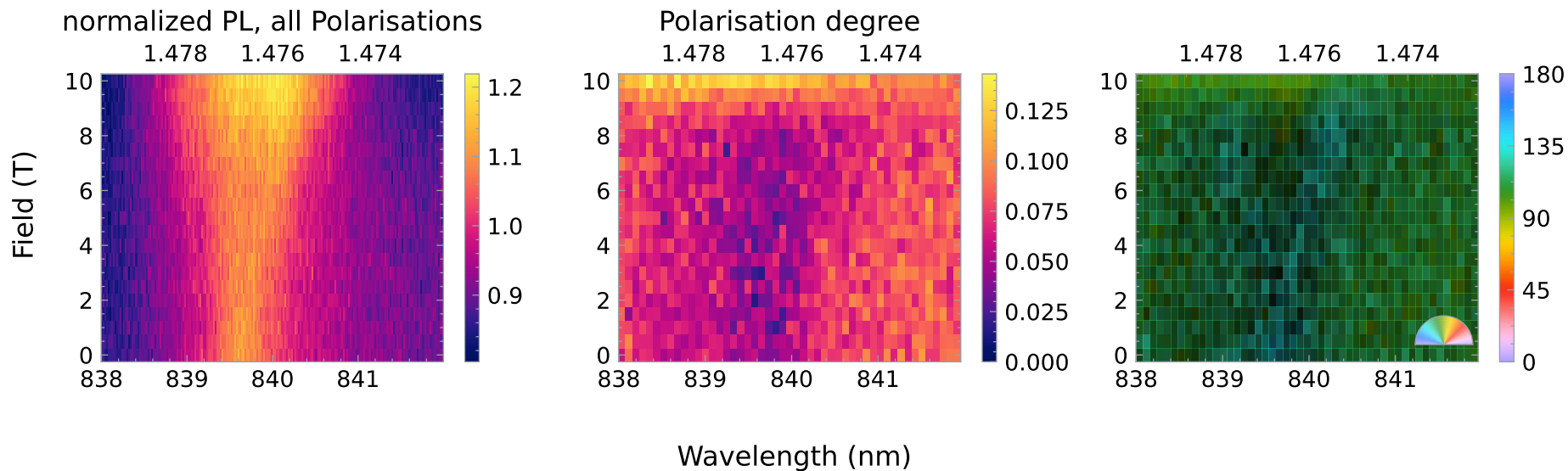
Polarisation degree



Wavelength (nm)

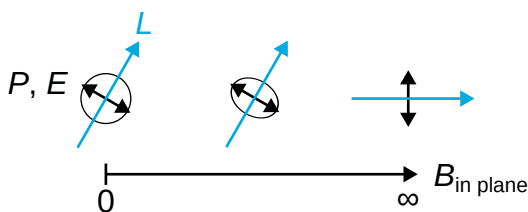
at 50K

2023-12-08\_LO\_MG\_NiPS3/d001\_flake04\_50K\_inPlane\_linPol\_sweepUp



# Understanding in Plane field

My measurement:



Based on Fig. 4 b in Spin-induced linear polarization of photoluminescence in antiferromagnetic van der Waals crystals, Nature Materials 2021

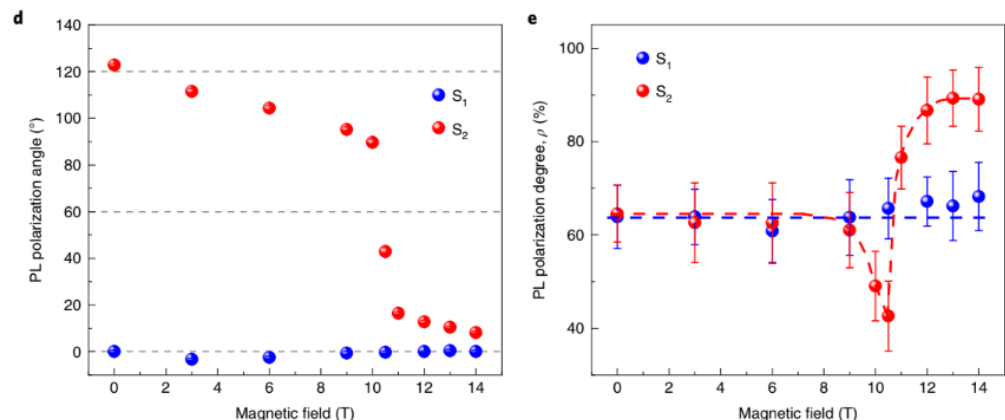
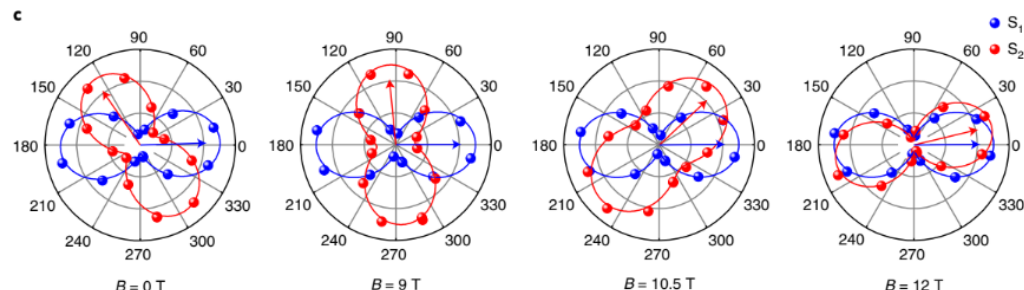
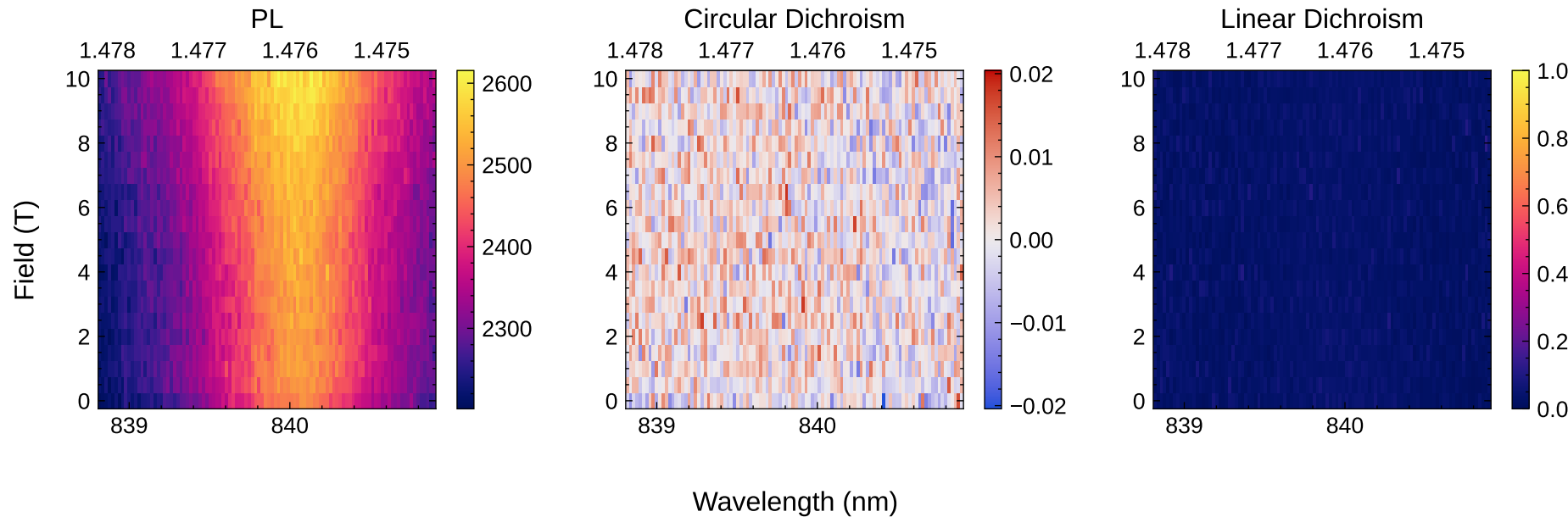


**Fig. 4 | Magnetic manipulation of PL polarization in the Voigt geometry.** **a**, Illustration of rotating linear polarization of peak X in an applied in-plane field. The solid orange, solid blue and hollow black arrows represent the Néel vector (**L**), electric dipole oscillator (**E**) and applied field (**B**), respectively. **b**, Illustrated diagram of the initial alignments of spins (thick blue and red arrows) and Néel vectors (thick orange arrows) in two samples. The crystal orientations (that is, the *a* axis) of two bulk NiPS<sub>3</sub> samples (S<sub>1</sub> and S<sub>2</sub>) are 120° from each other. **c**, Integrated PL intensity of peak X as a function of collection polarization angle on S<sub>1</sub> and S<sub>2</sub> at different magnetic fields ( $B=0, 9, 10.5$  and 12 T). **d**, PL polarization angles of sample S<sub>1</sub> and S<sub>2</sub> as a function of the in-plane magnetic field. The black dashed lines are the possible zigzag spin chain directions. **e**, Polarization degree,  $\rho=(I_b-I_a)/(I_b+I_a)$ , as a function of the applied magnetic field for S<sub>1</sub> and S<sub>2</sub>. The results show a magnetic phase transition around  $B=10.5$  T.

# Out of plane field



## Literature Review: Oct 2023

### Current Status

Materials

Setup

Photoluminescence and Reflection at 0 T

NiPS<sub>3</sub> in magnetic field

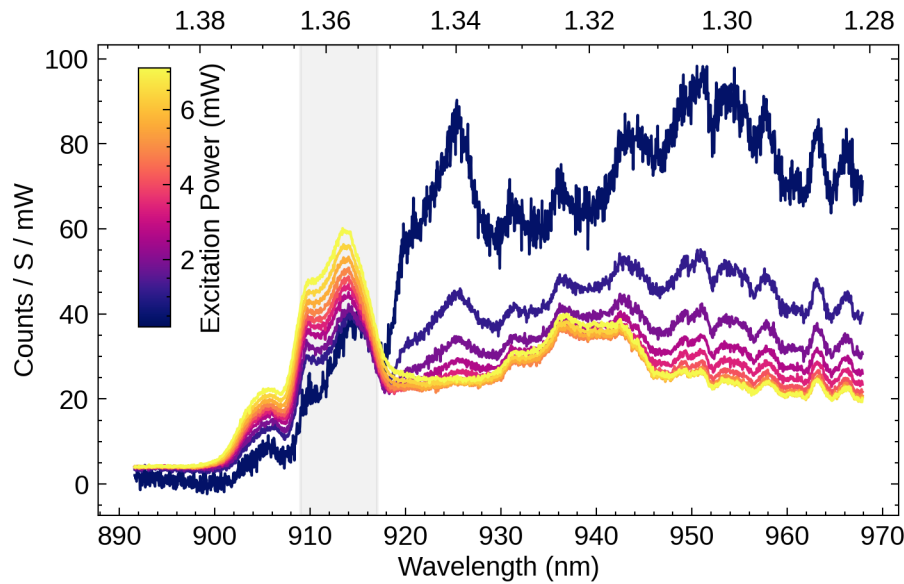
in plane

out of plane

CrPS<sub>4</sub>

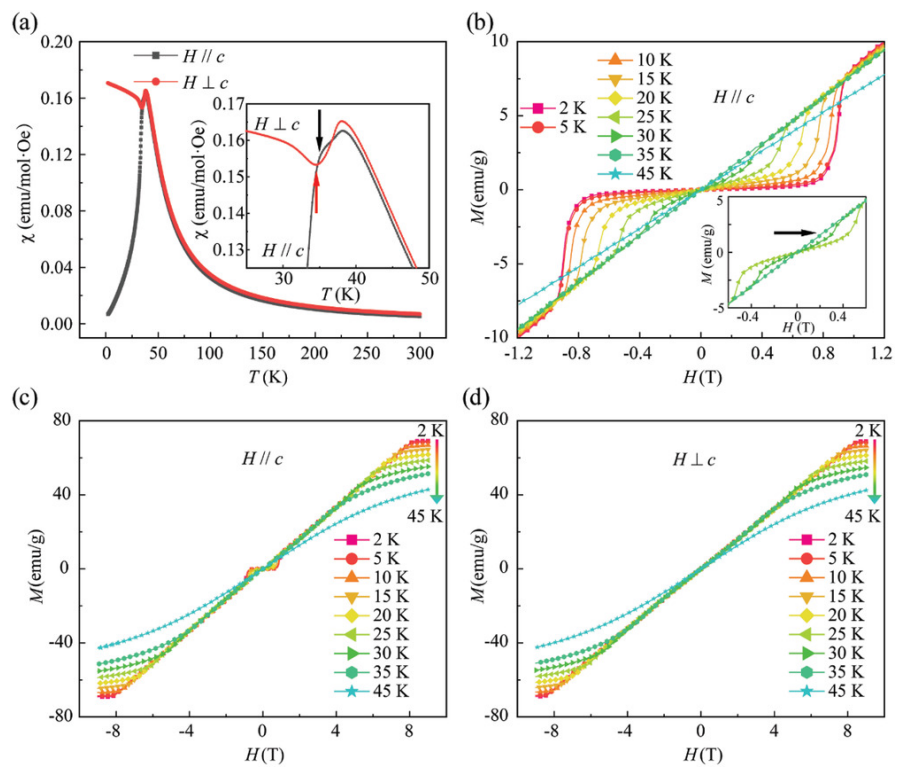
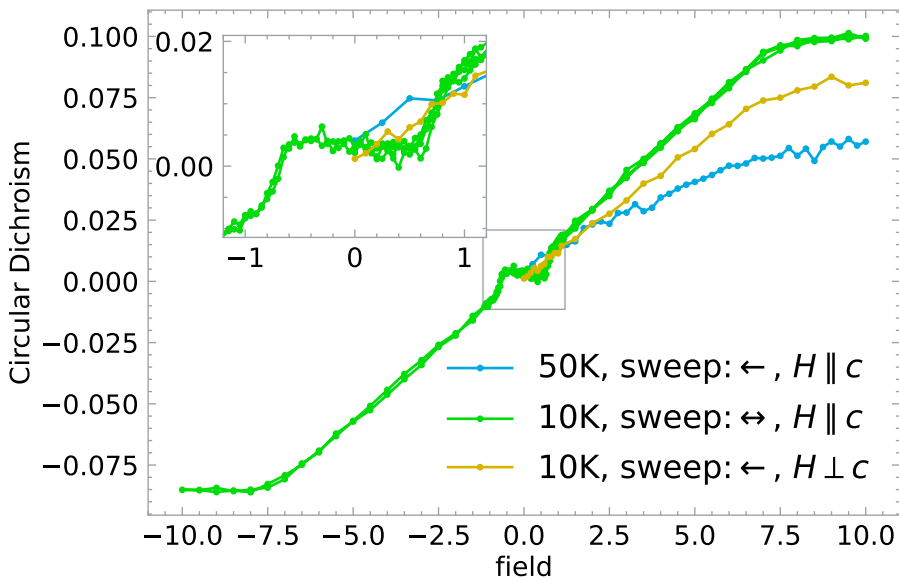
### Writing

## excitation power dependence



# CrPS<sub>4</sub>: CD $\propto M$ ?

My measurement:



Magnetic Structure and Metamagnetic Transitions in the van der Waals Antiferromagnet CrPS<sub>4</sub>, Advanced Materials 2020

# moving flakes

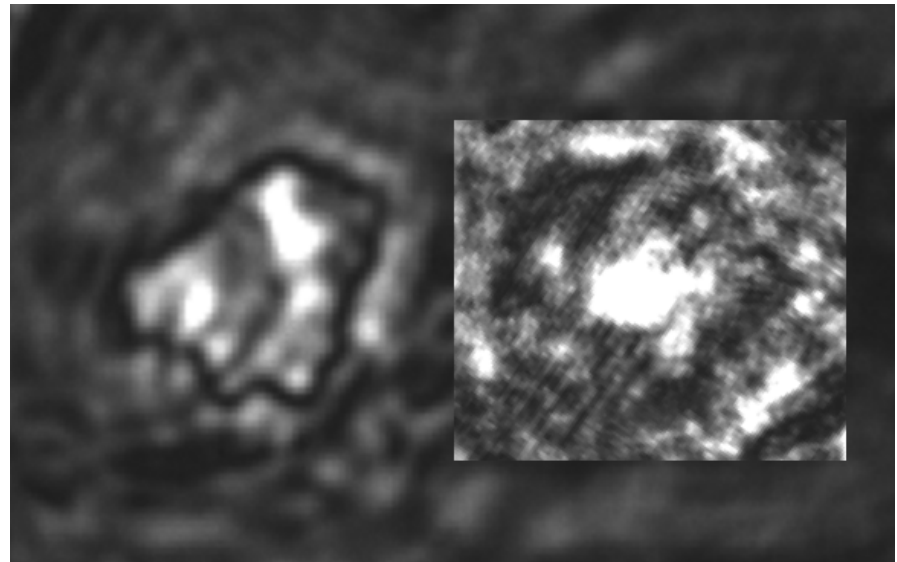
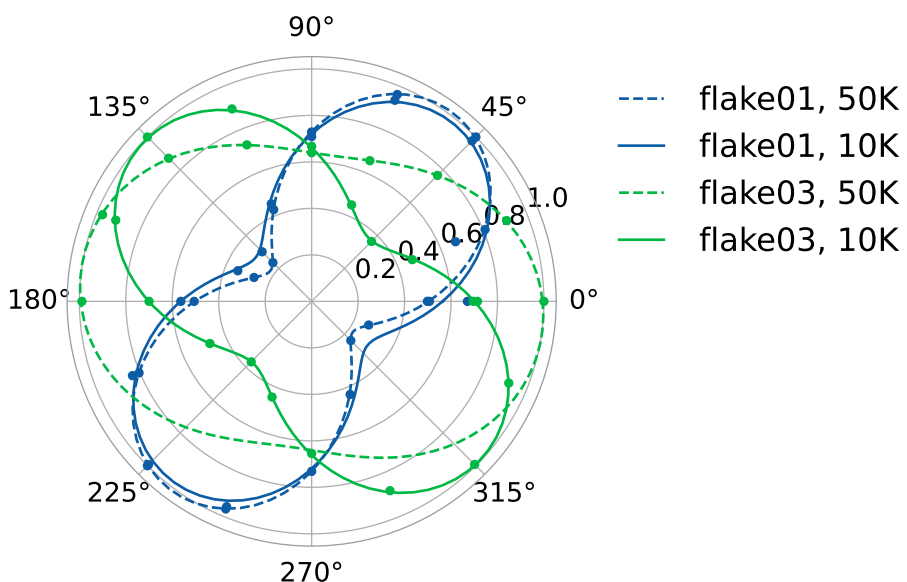
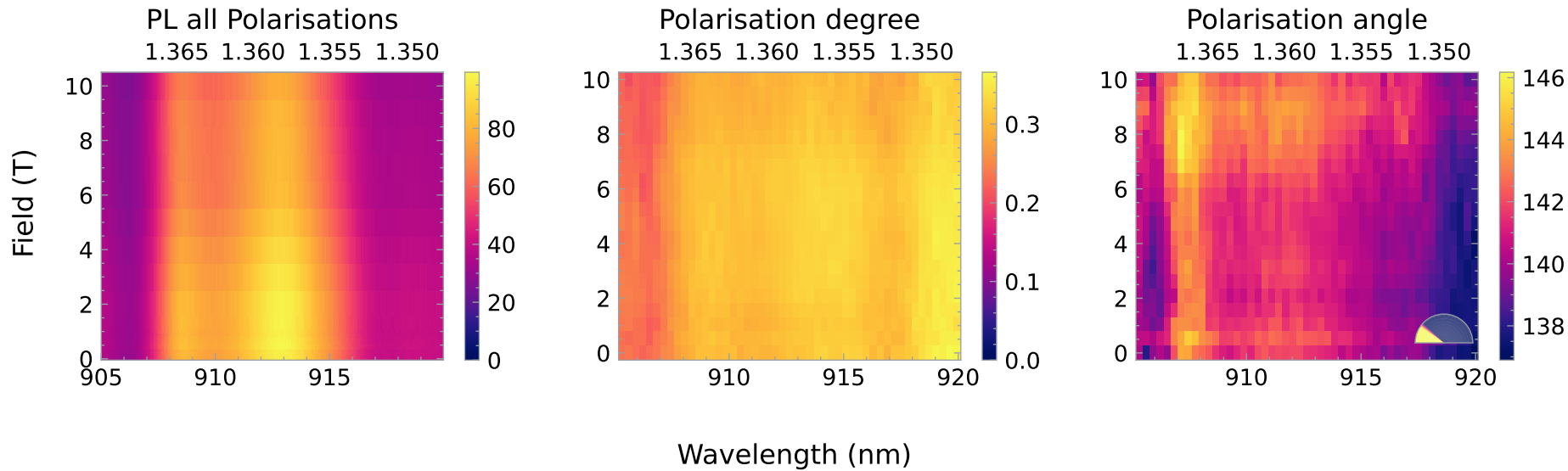


**Figure:** Flake 03, background: flake after cooldown, foreground: flake before, rotated by 30°

# Linear Polarisation

2023-12-15\_CrPS4\_inPlane/d001\_linPolDet\_circExcPol\_10K\_flake03\_4mW



## Literature Review: Oct 2023

### Current Status

Materials

Setup

Photoluminescence and Reflection at 0 T

NiPS<sub>3</sub> in magnetic field

in plane

out of plane

CrPS<sub>4</sub>

### Writing



